GEOPHYSICAL RESEARCH LETTERS, VOL. 35, L22106, doi:10.1029/2008GL035767, 2008

Discovery of a transient radiation belt at Saturn

E. Roussos,[1] N. Krupp,[1] T. P. Armstrong,[2] C. Paranicas,[3] D. G. Mitchell,[3] S. M. Krimigis,[3,4] G. H. Jones,[5,6] K. Dialynas,[7] N. Sergis,[4] and D. C. Hamilton[8]

Received 21 August 2008; revised 11 October 2008; accepted 15 October 2008; published 25 November 2008.

[1] Radiation belts have been detected in situ at five planets. Only at Earth however has any variability in their intensity been heretofore observed, in indirect response to solar eruptions and high altitude nuclear explosions. The Cassini spacecraft's MIMI/LEMMS instrument has now detected systematic radiation belt variability elsewhere. We report three sudden increases in energetic ion intensity around Saturn, in the vicinity of the moons Dione and Tethys, each lasting for several weeks, in response to interplanetary events caused by solar eruptions. However, the intensifications, which could create temporary satellite atmospheres at the aforementioned moons, were sharply restricted outside the orbit of Tethys. Unlike Earth, Saturn has almost unchanging inner ion radiation belts: due to Saturn's near-symmetrical magnetic field, Tethys and Dione inhibit inward radial transport of energetic ions, shielding the planet's main, inner radiation belt from solar wind influences. **Citation:** Roussos, E., N. Krupp, T. P. Armstrong, C. Paranicas, D. G. Mitchell, S. M. Krimigis, G. H. Jones, K. Dialynas, N. Sergis, and D. C. Hamilton (2008), Discovery of a transient radiation belt at Saturn, *Geophys. Res. Lett.*, *35*, L22106, doi:10.1029/2008GL035767.

1. MeV Ions in the Innermost Magnetosphere

[2] Ions with energies >1 MeV/nuc were first sampled in Saturn's radiation belts during the Pioneer 11 and Voyager 1 and 2 flybys [*Fillius and McIlwain*, 1980; *McDonald et al.*, 1980; *Van Allen et al.*, 1980; *Vogt et al.*, 1982]. A similar spatial distribution to what these three spacecraft detected was recorded by MIMI/LEMMS [*Krimigis et al.*, 2004] in July 2004, on Cassini's arrival at Saturn (Figure 1). MeV ion fluxes are identical during the orbit's inbound and outbound legs, consistent with local time symmetric MeV ion distribution [*Paranicas et al.*, 2008]. Inside the dipole $L \sim 5$, four distinct peaks can be identified. Between them, fluxes drop to instrument background levels. These minima are located at regions magnetically connected to large moons' orbits: Janus and Epimetheus, Mimas, and Enceladus. A more subtle dropout appears at $L \sim 2.8$, the distance of the G-ring, as discovered in the earlier observations, first modeled by *Van Allen* [1983], and now resampled repeatedly by Cassini [*Jones et al.*, 2006; *Hedman et al.*, 2007]. These correlations leave no doubt that absorption by moons and ring material is responsible for ion depletions. These peaks' outer boundary is located close to Tethys' L-shell, at 4.89 R_s. Beyond that distance, LEMMS typically measures background at the energies of concern. Tethys' orbit is likely a transitional region between where particle losses dominate and one in which sources prevail.

2. Dione Belt: A New Radiation Belt Component

[3] Deviations from this typical picture described in the previous section were first observed by Cassini during the day 47–48, 2005 periapsis pass (Figure 1, turquoise curve). MeV ion fluxes rose above background between the orbit of Tethys and ~8 R_s, a region encompassing Dione's L-shell around 6.3 R_s, both inbound and outbound. This indicated the presence of a new, local-time symmetric radiation belt, from hereon called the Dione Belt. The peak flux measured therein was ~20 times higher than the LEMMS background at these energies. A partial flux dropout was observed at Dione's L-shell, suggesting that Dione absorbs some of these newly injected ions. A more dramatic dropout is observed at Tethys' L-shell, where fluxes reach background levels. Furthermore, ion fluxes inside Tethys' orbit are at typical levels. Simultaneous enhancements were observed at all ion energies down to few keV/nuc and in keV electrons, but here we primarily discuss MeV ion observations. The P2 channel is used as an indicator, as it has higher signal-to-noise ratio than the other MeV ion channels. Similar results are obtained using all LEMMS higher energy channels than P2, where the Dione Belt is visible (up to ~10 MeV).

[4] The Dione belt was again observed during the next periapsis passage, on day 68, 2005 (Figure 1, yellow curve). Its peak had moved inward and its maximum flux had decayed by a factor of 4. The depletion at Tethys' L-shell was still persistent and again, no variation was seen in the innermost magnetosphere's MeV-range ion fluxes. This is consistent with ions diffusing radially inwards and subsequently being depleted by Tethys as they drift around Saturn within that moon's sweeping corridor. Low radial diffusion rates, as inferred [*Van Allen*, 1983; *Cooper*, 1983; *Roussos et al.*, 2007], could account for large ion lifetimes at that distance and provide sufficient time for a flux tube to completely drain of energetic ions through repeated moon encounters. Also, as MeV ions drift around the planet significantly quicker than the cold plasma [*Thomsen and Van Allen*, 1980], trapped MeV ions near a moon's orbital

[1]Max-Planck-Institut für Sonnensystemforschung, Katlenburg-Lindau, Germany.
[2]Fundamental Technologies, LLC, Lawrence, Kansas, USA.
[3]Applied Physics Laboratory, Johns Hopkins University, Laurel, Maryland, USA.
[4]Office of Space Research and Technology, Academy of Athens, Athens, Greece.
[5]Mullard Space Science Laboratory, Department of Space and Climate Physics, University College London, Dorking, UK.
[6]Centre for Planetary Sciences, University College London, London, UK.
[7]Section of Astronomy, Astrophysics and Mechanics, Department of Physics, University of Athens, Zografos, Greece.
[8]Physics Department, University of Maryland, College Park, Maryland, USA.

0094-8276/08/2008GL035767

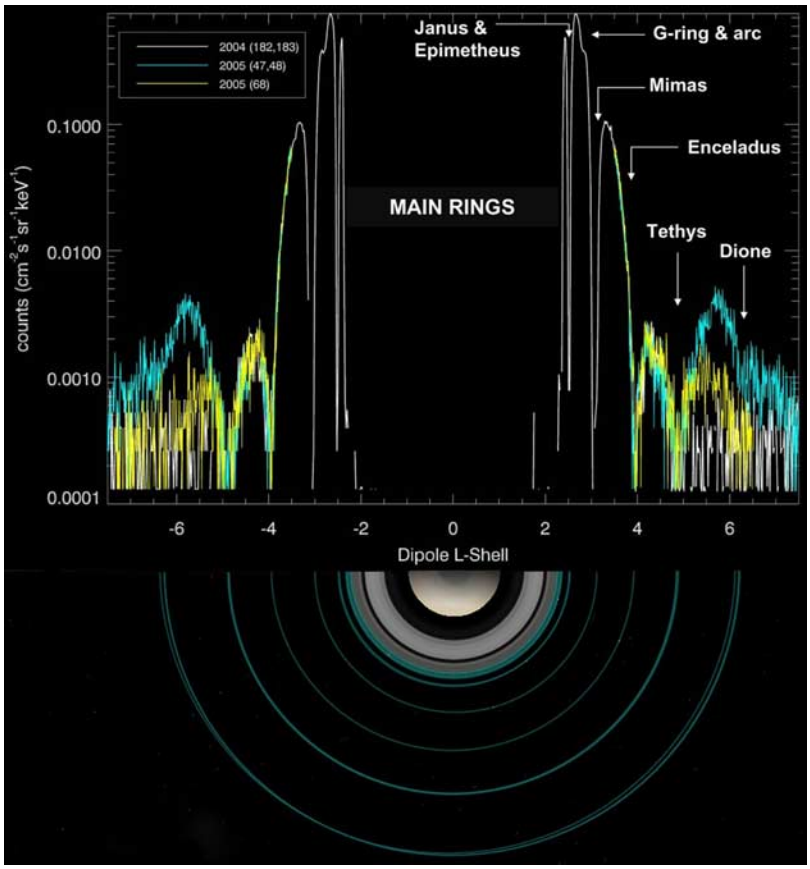

Figure 1. Differential ion fluxes from the LEMMS P2 ion channel (2.28–4.49 MeV/nuc) as a function of dipole L-shell. Negative L denotes the inbound part of the orbit, positive outbound. The 2004 profile (white curve) is the most common, identified in 27 out of the 36 orbits considered in this study. Several moons' and rings' L-shells are indicated. The lowest background is measured above the main rings that absorb all energetic ions, while Saturn's volume and the strong dipole field "shadow" instrument-penetrating, galactic cosmic rays. The two 2005 profiles (yellow and turquoise), correspond to orbits with periapsis at L = 3.5 reveal a flux enhancement centered close to Dione's L-shell (the Dione belt). The enhancement exists only outside Tethys' L-shell.

distance re-encounter the body frequently and have high probabilities of striking its surface [*McDonald et al.*, 1980].

[5] The Dione belt was still present in the third successive periapsis passage (day 89, 2005), but no longer visible on the following orbit (day 104, 2005). The belt reappeared on day 232 of 2005 and in the next orbit the flux decay and inward-moving peak flux were again identified. However, during the following periapsis (days 266–267/2005), fluxes intensified, reaching the highest values observed in this region during Cassini's mission to date. The Dione belt then decayed, and was last observed for a few days before the end of 2005. We observe that two interplanetary disturbances hit Saturn's magnetosphere before the two appearances of this transient radiation belt and one just before that belt's intensification. Figure 2 shows the detection of these events, where the P2 channel is used as a storm indicator, given the sparsity of MeV ions in the solar wind during quiet times. It is clear that solar energetic particle events are linked to the Dione belt, though undetermined is whether these particles enter the magnetosphere directly and diffuse inwards, or that the interplanetary disturbances accelerate magnetospheric particles to MeV energies [*Hudson et al.*, 1995]. We note that the Pioneer 11 Saturn flyby occurred during an interplanetary disturbance; the Dione belt was present, consistent with the LEMMS observations [*McDonald et al.*, 1980] (Figures 1 and 3).

3. Dione Belt Implications

[6] A transient radiation belt's presence has important implications for several Saturnian magnetospheric processes. The Dione belt lies within Saturn's dense neutral cloud [*Jurac and Richardson*, 2005]. Any associated enhancement of energetic electron fluxes will increase the electron temperature, and consequently, the electron impact ionization rates. Overall, the Dione belt should increase the plasma mass loading rate that results from the neutral cloud's erosion. In addition, the suprathermal proton pressure appears considerably increased compared to the usually measured values, indicating that the keV particles, and consequently the ring current, are also affected by the solar storm hitting the magnetosphere, as shown in Figure 3: the energetic ion pressure appears unusually high compared to typical values measured in the plotted L-range, during an intense Dione belt outbound pass of the day 267/2005.

[7] Enhanced energetic ion and electron fluxes will also increase the surface irradiation of Tethys, Dione and Rhea, potentially generating transient, sputter-produced atmos-

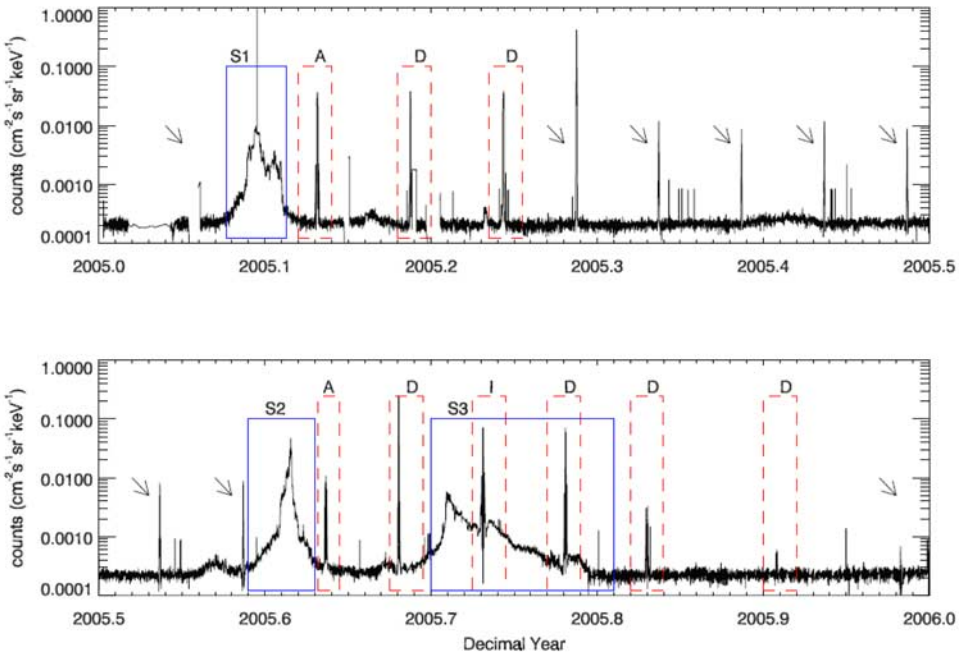

Figure 2. LEMMS MeV ion flux long term plots for 2005, showing two successive 6-month time series of P2 differential fluxes. Spikes are the rapid periapsis crossings through the radiation belts. Between periapses, Cassini is in the outer magnetosphere, the magnetosheath, or the solar wind. The three solar energetic particle events discussed are indicated by S1, S2 and S3. S1 was also detected near Earth, about 10 days earlier [*Foullon et al.*, 2007], as the Sun, Earth, and Saturn were almost aligned. Boxes identify the orbits when the Dione Belt was present, with the letters "A", "I" and "D" denoting the belts' appearance, intensification or decay, respectively. Arrows indicate periapses when the Dione belt was absent. The remaining spikes probably correspond to single galactic cosmic ray hits on the instrument.

pheres of those moons. Cassini close flybys of Tethys and Dione, on days 267 and 284, respectively, occurred when the Dione belt was intense. Using MIMI/CHEMS and LEMMS ion flux and composition data in the 3 keV/nuc to 10 MeV/nuc range, we estimate that the energetic ion contribution to Dione surface sputtering rates increases by about one order of magnitude, to [1 ± 0.5] 10^{23} neutrals/s. This is when comparing the highest fluxes yet observed, on day 267, to cases where the belt was absent. This number is lower than earlier estimations based on Voyager data [e.g., *Jurac et al.*, 2001], not considering, however, the contribution from the cold plasma.

[8] The Cassini mission has to date been active at Saturn during solar minimum. Given its origin, the Dione belt might represent a near-permanent but highly variable feature during solar maximum, resulting in all the aforementioned effects being significantly enhanced.

4. Ionic Radiation Belts Inside Tethys' Orbit

[9] Unlike the Dione belt, the ion belts within Tethys' L-shell seem very stable. To further prove their stability, peak MeV ion fluxes from the four regions inside Tethys' L-shell from July 2004 until January 2008 were monitored (Figure 4). Dione belt fluxes change by up to a factor of 100, while inner belt flux variation was less than a factor of 2. These small variations showed no correlation to the Dione belt, unlike the slot region separating Earth's inner and the outer radiation belts that can partially fill with energetic particles during large solar storms [*Baker et al.*, 2004]. This means that Tethys presents a "strong" obstacle against inward radial transport of MeV ions and that the inner belts are indeed stable and isolated.

[10] Thanks to this stability, it is possible to construct flux maps of Saturn's inner belts, by assembling different parts

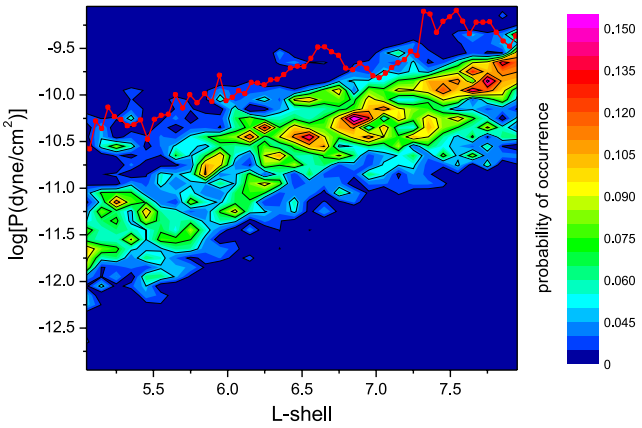

Figure 3. Radial pressure profile for the energetic (E > 3 keV) protons, measured during the equatorial plane orbits of Cassini (days 265/2005 to 182/2006). The data are statistically weighted to compensate for the uneven radial coverage. The color is the occurrence probability per $dL \times dlogP$ bin. The radial resolution is $dL = 0.1$ R_S. The red line superimposed to the probability map corresponds to the pressure values measured during the outbound Cassini pass on day 267 of 2005.

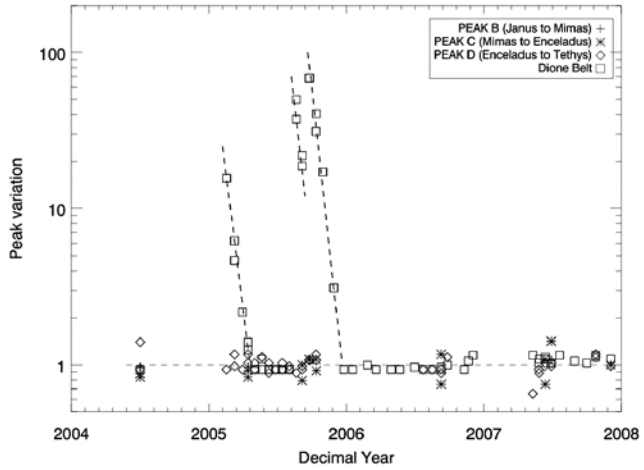

Figure 4. Monitoring of P2 channel differential fluxes in three of the four inner belts' permanent peaks (Figure 1) and in the Dione belt. The peak between the main rings and Janus and Epimetheus' orbits is not included, as it was sampled only once. Data correspond to the maximum of each peak and are extracted when this is resolved. Fluxes are normalized to an average flux when the Dione belt was absent and to the same equatorial pitch angle. Decay slopes of the Dione belt (dashed lines) are similar in all three cases.

of the angular and L-shell distribution from different orbits. Figure 5 shows a resulting map, where latitudinal, local time symmetry for a given L-shell, and an undisturbed dipole field are assumed. Similar maps can be created for other energy ranges of ions above 1 MeV. Note that fluxes do not reach background at the L-range of Janus and Epimetheus, meaning that MeV ion populations can be partly transported across the two moons' shared orbit.

5. Source of the Inner Belts' MeV Ions

[11] As concluded earlier, the ionic radiation belt of Saturn cannot be populated by inward radial diffusion; diffusion is therefore secondary to losses to Tethys. In addition, Saturn's neutral gas cloud, whose density peaks inside Rhea's orbit (L = 8.74), leads to strong ion losses in the <100 keV range due to charge-exchange reactions [*Paranicas et al.*, 2008]. Moons and the neutral gas cloud together form an effective energy filter for ions that diffuse towards Saturn's inner magnetosphere.

[12] The inner belt MeV ion population's stability requires a stable source. Any process involving the outer magnetosphere cannot be responsible for populating the inner belts (e.g., diffusion of 100-keV to ~1-MeV ions or double charge exchange). For energies above 10 MeV/nuc, the proposed source mechanism is the CRAND process, also responsible for very energetic protons in Earth's inner radiation belt. During this process GeV cosmic rays impacting Saturn's atmosphere or rings produce neutrons that then decay to protons with energies >10 MeV, becoming trapped in the magnetosphere. This suggested process's signature is a peak in the energy-flux spectrum, centered around 20 MeV/nuc, in both the LEMMS dataset and in that of previous missions [*Blake et al.*, 1983].

[13] However, given the inner radiation belts' isolation, no obvious source exists for 1–10 MeV ions. At Earth, such ions are partly attributed to light element isotopes (deuterium, tritium, Helium-3 and 4) that result from the nuclear collisions of CRAND protons in our planet's neutral atmosphere [*Selesnick and Mewaldt*, 1996]. This may also occur at Saturn and may be enhanced by the neutral gas cloud, the

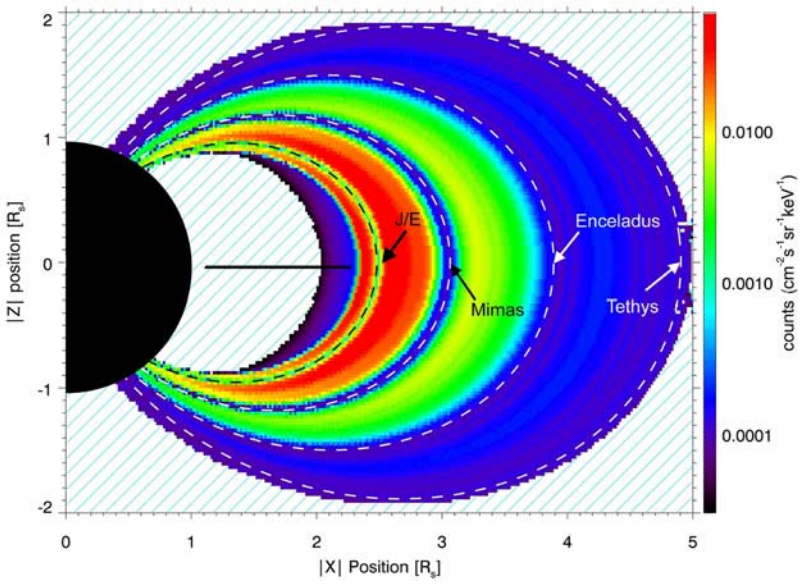

Figure 5. Differential flux map of the stable belts inside Tethys' L-shell of the 25–60 MeV/nuc ions, based on LEMMS data from 36 orbits. The L-shells of the various moons, are indicated. The partial flux dropout at the shell of the G-ring is also visible. Hatched regions above the main rings have particle flux lower or equal to that of the color bar. The radiation belt inside the D-ring [*Krimigis et al.*, 2005] is not presented here.

E- and G-rings. We note that 1–10 MeV ions occupy exactly the same region as the >10 MeV ions, which may signify an association between the two populations. Alternatively, these ions could be trapped, anomalous cosmic ray products [*Selesnick et al.*, 1995]. Both processes are consistent with the stable source requirement, but since LEMMS has limited plasma composition determination we are not in a position at this stage to privilege one or the other of these possibilities.

[14] **Acknowledgments.** The authors thank M. Fränz and A. Lagg (MPS) for support in software development, M. Kusterer (JHUAPL) for data reduction. MIMI/LEMMS was part-financed by the German Bundesministerium für Bildung und Forschung through the German Aerospace Centre (DLR) and by the Max Planck Gesellschaft. Work at JHUAPL was supported by NASA. GHJ is supported by a UK STFC Advanced Fellowship.

References

Baker, D. N., S. G. Kanekal, X. Li, S. P. Monk, J. Goldstein, and J. L. Burch (2004), An extreme distortion of the Van Allen belt arising from the 'Halloween' solar storm in 2003, *Nature*, *432*, 878–881.

Blake, J. B., H. H. Hilton, and S. H. Margolis (1983), On the injection of cosmic ray secondaries into the inner Saturnian magnetosphere: 1. Protons from the CRAND process, *J. Geophys. Res.*, *88*, 803–807.

Cooper, J. F. (1983), Nuclear cascades in Saturn's rings: Cosmic ray albedo neutron decay and origins of trapped protons in the inner magnetosphere, *J. Geophys. Res.*, *88*, 3945–3954.

Fillius, W., and C. McIlwain (1980), Very energetic protons in Saturn's radiation belt, *J. Geophys. Res.*, *85*, 5803–5811.

Foullon, C., C. J. Owen, S. Dasso, L. M. Green, I. Dandouras, H. A. Elliott, A. N. Fazakerley, Y. V. Bogdanova, and N. U. Crooker (2007), Multi-spacecraft study of the 21 January 2005 ICME, *Sol. Phys.*, *244*, 139–165, doi:10.1007/s11207-007-0355-y.

Hedman, M. M., J. A. Burns, M. S. Tiscareno, C. C. Porco, G. H. Jones, E. Roussos, N. Krupp, C. Paranicas, and S. Kempf (2007), The source of Saturn's G Ring, *Science*, *317*, 653–656.

Hudson, M. K., A. D. Kotelnikov, X. Li, I. Roth, M. Temerin, J. Wygant, J. B. Blake, and M. S. Gussenhoven (1995), Simulation of proton radiation belt formation during the March 24, 1991 SSC, *Geophys. Res. Lett.*, *22*, 291–294.

Jones, G. H., E. Roussos, N. Krupp, C. Paranicas, J. Woch, A. Lagg, D. G. Mitchell, S. M. Krimigis, and M. K. Dougherty (2006), Enceladus' varying imprint on the magnetosphere of Saturn, *Science*, *311*, 1412–1415.

Jurac, S., and J. D. Richardson (2005), A self-consistent model of plasma and neutrals at Saturn: Neutral cloud morphology, *J. Geophys. Res.*, *110*, A09220, doi:10.1029/2004JA010635.

Jurac, S., R. E. Johnson, J. D. Richardson, and C. Paranicas (2001), Satellite sputtering in Saturn's magnetosphere, *Planet. Space Sci.*, *49*, 319–326.

Krimigis, S. M., et al. (2004), Magnetospheric Imaging Instrument (MIMI) on the Cassini mission to Saturn/Titan, *Space Sci. Rev.*, *114*, 233–329.

Krimigis, S. M., et al. (2005), Dynamics of Saturn's magnetosphere from MIMI during Cassini's orbital insertion, *Science*, *307*, 1270–1273.

McDonald, F. B., A. W. Schardt, and J. H. Trainor (1980), If you've seen one magnetosphere you haven't seen them all: Energetic particle observations in the Saturn magnetosphere, *J. Geophys. Res.*, *85*, 5813–5830.

Paranicas, C., et al. (2008), Sources and losses of energetic protons in Saturn's magnetosphere, *Icarus*, *197*, 519–525, doi:10.1016/j.icarus.2008.05.011.

Roussos, E., G. H. Jones, N. Krupp, C. Paranicas, D. G. Mitchell, A. Lagg, J. Woch, U. Motschmann, S. M. Krimigis, and M. K. Dougherty (2007), Electron microdiffusion in the Saturnian radiation belts: Cassini MIMI/LEMMS observations of energetic electron absorption by the icy moons, *J. Geophys. Res.*, *112*, A06214, doi:10.1029/2006JA012027.

Selesnick, R. S., and R. A. Mewaldt (1996), Atmospheric production of radiation belt light isotopes, *J. Geophys. Res.*, *101*, 19,745–19,757.

Selesnick, R. S., A. C. Cummings, J. R. Cummings, R. A. Mewaldt, E. C. Stone, and T. T. von Rosenvinge (1995), Geomagnetically trapped anomalous cosmic rays, *J. Geophys. Res.*, *100*, 9503–9518.

Thomsen, M. F., and J. A. Van Allen (1980), Motion of trapped electrons and protons in Saturn's inner magnetosphere, *J. Geophys. Res.*, *85*, 5831–5834.

Van Allen, J. A. (1983), Absorption of energetic protons by Saturn's Ring G, *J. Geophys. Res.*, *88*, 6911–6918.

Van Allen, J. A., M. F. Thomsen, B. A. Randall, R. L. Rairden, and C. L. Grosskreutz (1980), Saturns' magnetosphere, rings, and inner satellites, *Science*, *207*, 415–421.

Vogt, R. E., D. L. Chenette, A. C. Cummings, T. L. Garrard, E. C. Stone, A. W. Schardt, J. H. Trainor, N. Lal, and F. B. McDonald (1982), Energetic charged particles in Saturn's magnetosphere: Voyager 2 results, *Science*, *215*, 577–582.

T. P. Armstrong, Fundamental Technologies, LLC, 2411 Ponderosa Drive, Lawrence, KS 66044, USA.

K. Dialynas, Section of Astronomy, Astrophysics and Mechanics, Department of Physics, University of Athens, Panepistimiopolis, GR-157 84 Zografos, Greece.

D. C. Hamilton, Physics Department, University of Maryland, College Park, MD 20742, USA.

G. H. Jones, Mullard Space Science Laboratory, Department of Space and Climate Physics, University College London, Holmbury St. Mary, Dorking, Surrey RH5 6NT, UK.

S. M. Krimigis, C. Paranicas, and D. G. Mitchell, Applied Physics Laboratory, Johns Hopkins University, 11100 Johns Hopkins Road, Laurel, MD 20723, USA.

N. Krupp and E. Roussos, Max-Planck-Institut für Sonnensystemforschung, Max-Planck-Str. 2, D-37191 Katlenburg-Lindau, Germany. (roussos@mps.mpg.de)

N. Sergis, Office of Space Research and Technology, Academy of Athens, Soranou Efesiou 4, Papagos, GR-115 27 Athens, Greece.